Boundary states in the open string channel and CFT near a corner

Yosuke IMAMURA[1,*)], Hiroshi ISONO[2,**)] and Yutaka MATSUO[3,***)]

Department of Physics, Faculty of Science, University of Tokyo
Hongo 7-3-1, Bunkyo-ku, Tokyo 113-0033, Japan

We generalize the idea of boundary states to the open string channel. They describe emission and absorption of open strings in the presence of intersecting D-branes. We construct the explicit oscillator representation for the free boson and fermionic ghost. The inner product of such states describes a disk amplitude of rectangular shape and possesses modular covariance with a nontrivial conformal weight. We compare the result obtained here with those obtained using two different methods, one employing the path integral formalism and one employing the conformal anomaly. We find that all these methods give consistent results. In our method, we must be careful in our treatment of the singularity of the CFT near the corners. Specifically, we derive the correction to the conformal weight of the primary field inserted at the corner, and it gives the modular weight of the rectangle amplitude. We also carry out explicit computations of the correlation functions.

§1. Introduction

A boundary state[1),2)] is one of the most fundamental objects in the boundary conformal field theory. It encodes the effect of the boundary conditions in the operator formalism on a 2D world sheet. In string theory, it gives an exact description of D-brane by specifying how a closed string is emitted or absorbed by the D-brane.

In the language of 2D conformal field theory, the boundary state is characterized by the relation

$$T_{\sigma\tau}|B^c\rangle = 0, \tag{1.1}$$

or in the Fourier modes of the Virasoro algebra,

$$(L_n - \tilde{L}_{-n})|B^c\rangle = 0 . \tag{1.2}$$

The superscript c is attached to indicate that this boundary state belongs to closed string Hilbert space. There have been many works studying various properties of such states. (For reviews, see, for example, Refs. 3)–10)).

As far as we know, the boundary state condition (1.1) has been considered only in the closed string channel. Such studies are natural, because the D-brane acts as a source of emission/absorption of closed strings, and the boundary state describes such a process. For example, the inner product of the boundary states $\langle B^c|q^{L_0+\tilde{L}_0-\frac{c}{12}}|B^c\rangle$ describes closed string propagation between D-branes. The contribution of massless closed string fields to this amplitude is identical to the potential derived using supergravity, and with this information, we can determine the tensions of D-branes.[11)]

---

*) E-mail: imamura@hep-th.phys.s.u-tokyo.ac.jp
**) E-mail: isono@hep-th.phys.s.u-tokyo.ac.jp
***) E-mail: matsuo@phys.s.u-tokyo.ac.jp

As we see below, however, it is also possible to consider a similar process for open strings. We consider the situation in which two D-branes Λ and Σ intersect. [*]
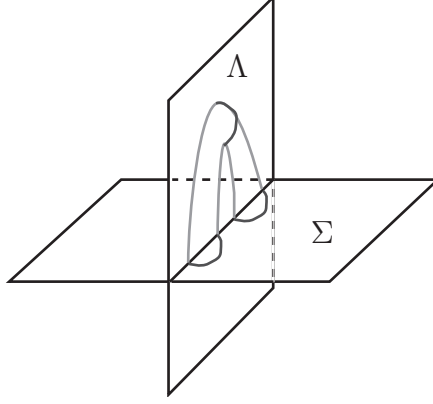Consider the physical process consisting of (1) an open string on a D-brane Λ being

Fig. 1.   An open string on the D-brane Λ is created/absorbed by another D-brane, Σ.

emitted from a D-brane Σ, (2) this open string propagating on the world volume of Λ and, (3) it being absorbed by Σ (see Fig.1). As the closed string amplitude, such a process would be described by an inner product of the boundary state as

$$\,^{\Sigma}_{\Lambda\Lambda}\langle B^o|q^{L_0^{\Lambda\Lambda}+a^{\Lambda\Lambda}}|B^o\rangle^{\Sigma}_{\Lambda\Lambda}\,, \tag{1·3}$$

where $|B^o\rangle^{\Sigma}_{\Lambda\Lambda}$ belongs to the open string Hilbert space with both ends on the D-brane Λ and $a^{\Lambda\Lambda}$ is the zero-point energy for the $\Lambda\Lambda$ sector. We refer to such states as *open boundary states* (OBS) [**]. The first purpose of this paper is to define such states and to give their explicit representation for free fields.

We next study some basic properties of such states. Firstly, the inner product given by (1·3) gives a string amplitude with rectangular worldsheet. In general, it is possible to use different boundary conditions at the four sides. While this worldsheet has the topology of a disk, it possesses a modular property that can be written schematically as

$$\,^{\Lambda_r}_{\Sigma_b,\Sigma_t}\langle B^o|\tilde{q}^{L_0^{\Sigma_t\Sigma_b}+a^{\Sigma_t\Sigma_b}}|B^o\rangle^{\Lambda_l}_{\Sigma_t,\Sigma_b} = t^{w(\Sigma_t|\Lambda_l,\Lambda_r|\Sigma_b)}\,^{\Sigma_t}_{\Lambda_r,\Lambda_l}\langle B^o|q^{L_0^{\Lambda_l\Lambda_r}+a^{\Lambda_l\Lambda_r}}|B^o\rangle^{\Sigma_b}_{\Lambda_l,\Lambda_r}\,, \tag{1·4}$$

where $q=e^{-\pi t}\,and\,\tilde{q}=e^{-\pi/t}$, for a real $t>0$. The symbol $|B^o\rangle^{\Sigma_b}_{\Lambda_l,\Lambda_r}$ represents OBS with two independent boundary conditions, Λ_r and Λ_s, at two sides. The quantity $w(\Sigma_t|\Lambda_l,\Lambda_r|\Sigma_b)$ is the modular weight associated with the rectangle. This modular property implies that the rectangle amplitude is described by modular forms, in contrast to the usual disk amplitude.

---

[*] Strictly speaking, in the analysis given in this paper, it is not necessary that Λ and Σ "intersect" in the usual geometrical sense. In fact, it is possible to define the open boundary state even if Λ (resp. Σ) is embedded in Σ (resp. Λ) or Λ and Σ are the same brane. The only condition which we need is that $\Sigma\cap\Lambda$ is not the null set.

[**] A partial result on OBS is announced in Ref. 12).

It is rather intriguing that the disk amplitude may have such a modular co-variance. We present two arguments from which this can be understood. The first is the most straightforward one, namely that regarding the evaluation of the path integral on the rectangle. Although we need to introduce a regularization, as usual, the amplitude is manifestly covariant, by definition, and is identical with the inner product of OBS.

Another argument, which is more illuminating, is that the rectangle amplitude is, strictly speaking, the same as the disk amplitude *with* four marked points on the boundaries. These points are mapped to the four corners of the rectangle. There is a relation between the cross ratio of the marked points with the modulus parameter t defined above. The conformal properties of CFT near the corner play an essential role. Specifically, we show that the modular weight $w(\Sigma_t|\Lambda_l, \Lambda_r|\Sigma_b)$ is the sum of the contributions from the corners.

We observe that the general behavior of CFT near the corner with a deficit angle results from the conformal anomaly of the stress-energy tensor. After we map from the disk amplitude, each corner has a primary insertion with a weight proportional to the central charge. When the boundary conditions of the neighboring sides are different, we also need to add a twist field. The modular weight $w(\Sigma_t|\Lambda_l, \Lambda_r|\Sigma_b)$ is proportional to the sum of the conformal weights of the inserted fields at each corner. We also must be careful in choosing the normal ordering of operators inserted at the corner. We show that near the corner, each operator effectively becomes two operators, as its mirror image also acts. We show this through explicit computation of the correlation function.

The organization of this paper is as follows. In §2, we give the definition of the boundary state in the open string channel. We then compute various rectangle amplitudes for the free boson case and derive their modular properties. In §3, in order to compare these amplitudes with those obtained using path integral computation, we study the general behavior of CFT at the corner with a deficit angle. In §4, we carry out the path integral evaluation of the rectangle amplitude. We present two equivalent computations, that employing the direct computation of the Laplacian on the rectangle and the derivation from the conformal anomaly. We find that both results coincide with that of the operator calculation through the open boundary states. In §5, we evaluate four point functions on the rectangle as an application of our formulation. These analyses are sufficient to establish various properties of the open boundary states.

After we submitted the first version of this paper to the arXiv, we were informed that the content of Ref. 13) partially overlaps that of this paper (in §2 and §§4.2). We improved the treatment of the stress energy tensor given in §2, following this reference.

§2.　Construction of the open boundary state

General formula

The definition of the open boundary state can be derived from the closed string sector (1·2) using the doubling technique. Let us consider the energy momentum tensor as the first example. We consider an open worldsheet of rectangular shape ($0 \leq \sigma \leq 2\pi, \tau \geq 0$). We identify the anti-holomorphic part of the energy-momentum tensor as

$$\bar{T}(\bar{w}) = T(2\pi - \bar{w}), \quad w = \sigma + i\tau, \tag{2·1}$$

which gives the condition at $w = \pi$. The combined tensor field $T(w, \bar{w}) = T(w) + \bar{T}(\bar{w})$ then satisfies the boundary condition (1·1) at the boundaries $\sigma = 0$ and $\sigma = \pi$. The boundary condition at $\tau = 0$ is

$$(T(\sigma) - T(-\sigma))|B^o\rangle = 0 \tag{2·2}$$

for $0 < \sigma < \pi$. We see below that care is needed at $\sigma = 0$ and $\sigma = \pi$ and indeed an anomaly exists there. This condition is reminiscent of the definition of the identity state in open string field theory,[16]

$$(T(\sigma) - T(\pi - \sigma))|I\rangle = 0. \tag{2·3}$$

In a sense, the relation between the OBS and the identity state is similar to that between the boundary state in the closed string channel and the crosscap state:[1] $|B^c\rangle \leftrightarrow |B^o\rangle$, $|C^c\rangle \leftrightarrow |I\rangle$.

In order to define the open boundary state, we have to specify three boundary conditions, two conditions at $\sigma = 0, \pi$ and one condition at $\tau = 0$. The first two, in general, are implemented by the doubling technique (for generic conformal fields ϕ and $\bar{\phi}$), represented by

$$\bar{\phi}_\alpha(\bar{w}) = (\Lambda_r)_{\alpha\beta}\phi_\beta(2\pi - \bar{w}), \tag{2·4}$$

and the periodicity of the chiral field ϕ_α,

$$\phi_\alpha(w + 2\pi) = G_{\alpha\beta}\phi_\beta(w). \tag{2·5}$$

Here, Λ_r or G are complex matrices. The boundary condition at $\sigma = 0$ is then specified by

$$\bar{\phi}_\alpha(\bar{w}) = (\Lambda_r G)_{\alpha\beta}\phi_\beta(-\bar{w}) \equiv (\Lambda_l)_{\alpha\beta}\phi_\beta(-\bar{w}). \tag{2·6}$$

This determines the monodromy matrix G in terms of $\Lambda_{l,r}$

$$G = (\Lambda_r)^{-1}\Lambda_l. \tag{2·7}$$

The boundary condition at $\tau = 0$ can be defined similarly as

$$\bar{\phi}_\alpha(\bar{w}) = (\Sigma_b)_{\alpha\beta}\phi_\beta(\bar{w}). \tag{2·8}$$

We need some consistency conditions in order to impose these conditions. For example, the consistency condition obtained by considering the vicinity of $w = 0$ is

$$\bar{\phi}(-\bar{w}) = \Sigma_b \cdot \phi(-\bar{w}) = \Sigma_b \cdot (\Lambda_l)^{-1} \cdot \bar{\phi}(\bar{w})$$
$$= \Lambda_l \cdot \phi(\bar{w}) = \Lambda_l \cdot (\Sigma_b)^{-1} \cdot \bar{\phi}(\bar{w}) \,, \tag{2·9}$$

which implies

$$\Sigma_b(\Lambda_l)^{-1} = \Lambda_l(\Sigma_b)^{-1} \quad \text{or} \quad (\Sigma_b(\Lambda_l)^{-1})^2 = 1 \,. \tag{2·10}$$

Similarly, the consistency condition obtained by considering the vicinity of $w = \pi$ is

$$\Sigma_b(\Lambda_r)^{-1} = \Lambda_r(\Sigma_b)^{-1} \quad \text{or} \quad (\Sigma_b(\Lambda_r)^{-1})^2 = 1 \,. \tag{2·11}$$

The definition of the boundary state can be written in terms of the chiral field alone. There are two equivalent ways to write the constraint on $|B^o\rangle_{\Lambda_l \Lambda_r}^{\Sigma_b}$,

$$\left(\phi_\alpha(-\sigma) - (\Lambda_l^{-1}\Sigma_b)_{\alpha\beta}\phi_\beta(\sigma) \right) |B^o\rangle_{\Lambda_l \Lambda_r}^{\Sigma_b} = 0 \,,$$
$$\left(\phi_\alpha(2\pi - \sigma) - (\Lambda_r^{-1}\Sigma_b)_{\alpha\beta}\phi_\beta(\sigma) \right) |B^o\rangle_{\Lambda_l \Lambda_r}^{\Sigma_b} = 0 \,. \tag{2·12}$$

Their equivalence can be shown trivially using (2·7).

Free bosons without a twist

Let us use a free boson (without a twist) in order to obtain the simplest explicit formula. The possible boundary conditions are those of the Neumann and Dirichlet types. In terms of $J(w) = \partial X(w)$, they can be written as

$$J(-\bar{w}) + \epsilon \bar{J}(\bar{w}) = 0 \,, \quad \text{at } \operatorname{Re}(w) = 0 \,. \tag{2·13}$$

Here we have $\epsilon = 1$ for Neumann and $\epsilon = -1$ for Dirichlet boundary condition. Employing the same notation as in our general discussion, the reflection matrices are identified as $\Lambda_{r,l} = -\epsilon$. Because we have $G = \epsilon_l \epsilon_r$, the chiral field is periodic when $\epsilon_l = \epsilon_r$ and anti-periodic when $\epsilon_l = -\epsilon_r$. The well-known free boson mode expansions are,

$$X^{(NN)}(w, \bar{w}) = \hat{x} - \alpha'\hat{p}(w - \bar{w}) + i\left(\frac{\alpha'}{2}\right)^{\frac{1}{2}} \sum_{m \neq 0} \frac{1}{m}\alpha_m(e^{imw} + e^{-imw}) \,, \tag{2·14}$$

$$X^{(DD)}(w, \bar{w}) = x + \frac{y - x}{2\pi}(w + \bar{w}) + i\left(\frac{\alpha'}{2}\right)^{\frac{1}{2}} \sum_{m \neq 0} \frac{1}{m}\alpha_m(e^{imw} - e^{-imw}) \,, \tag{2·15}$$

$$X^{(DN)}(w, \bar{w}) = x + i\left(\frac{\alpha'}{2}\right)^2 \sum_{r \in Z+1/2} \frac{1}{r}\alpha_r(e^{irw} - e^{-ir\bar{w}}) \,, \tag{2·16}$$

$$X^{(ND)}(w, \bar{w}) = x + i\left(\frac{\alpha'}{2}\right)^2 \sum_{r \in Z+1/2} \frac{1}{r}\alpha_r(e^{irw} + e^{-ir\bar{w}}) \,. \tag{2·17}$$

The commutation relations for the mode variables are

$$[\alpha_n, \alpha_m] = n\delta_{n+m,0} \,, \quad [\hat{x}, \hat{p}] = i \,. \tag{2·18}$$

We note that the zero mode sector is nontrivial only for NN.

The condition for the boundary state can be written in a form similar to that for the closed string case:

$$\partial_\tau X(\sigma,\tau)|_{\tau=0}|B^o\rangle^N_{\Lambda_l\Lambda_r} = 0, \qquad \partial_\sigma X(\sigma,\tau)|_{\tau=0}|B^o\rangle^D_{\Lambda_l\Lambda_r} = 0. \qquad (2\cdot19)$$

The only difference between the open and closed string cases is that the mode expansion depends on the boundary conditions for open strings and we have only one set of oscillators instead of two (the left and right mover).

The open boundary states are obtained by solving (2·19). The result can be written compactly as

$$|B^o\rangle^{\epsilon_b}_{\epsilon_l\epsilon_r} \propto \exp\left(-\epsilon_l\epsilon_b \sum_{n>0} \frac{1}{2n}\alpha^2_{-n}\right)|\text{zero mode}\rangle^{\epsilon_b}_{\epsilon_l,\epsilon_r}. \qquad (2\cdot20)$$

Here, $\epsilon_{l,r,b}$ represent the boundary conditions at the left, right and bottom, respectively, and are $+1$ for Neumann boundary conditions and -1 for Dirichlet boundary conditions. The sum is over all positive integers when $\epsilon_l = \epsilon_r$ and all half odd positive integers when $\epsilon_l \neq \epsilon_r$. The vacuum state $|\text{zero mode}\rangle^{\epsilon_b}_{\epsilon_l,\epsilon_r}$ is the simple Fock vacuum when $(\epsilon_l,\epsilon_r) \neq (+1,+1)$. For $(\epsilon_l,\epsilon_r) = (+1,+1)$, we need to prepare the zero mode wave function. An appropriate choice is $|\hat{p}=0\rangle$ for $\epsilon_b = 1$ and $|\hat{x}=x_0\rangle$ with $x_0 \in \mathbf{R}$ for $\epsilon_b = -1$.

Anomalies at the corners

Let us study the condition (2·2) in our specific constructions. It would be replaced by the condition

$$(L_n - L_{-n})|B\rangle^{\epsilon_b}_{\epsilon_l\epsilon_r} \overset{?}{=} 0. \qquad (2\cdot21)$$

It turns out, however, that we have an extra term if we apply the Virasoro generators $(n \neq 0)$ in terms of oscillators,

$$L_n = \frac{1}{2}\sum_m \alpha_{n-m}\alpha_m \qquad (2\cdot22)$$

where m runs over all integers for NN and DD boundary conditions and all half odd integers for DN and ND boundary conditions. With this extra term, we obtain, instead of (2·21),

$$(L_n - L_{-n} + (d_n)^{\epsilon_b}_{\epsilon_l\epsilon_r})|B\rangle^{\epsilon_b}_{\epsilon_l\epsilon_r} = 0, \qquad (2\cdot23)$$

where

$$(d_n)^{\epsilon_b}_{\epsilon_l\epsilon_r} = -2n(\lambda_l + (-1)^n\lambda_r), \quad \text{with} \quad \lambda_l = -\frac{\epsilon_b\epsilon_l}{16}, \ \lambda_r = -\frac{\epsilon_b\epsilon_r}{16}. \qquad (2\cdot24)$$

We show below that the quantities $\lambda_{l,r}$ are the conformal weights of the operators inserted at the corners. The meaning of this anomaly term becomes clearer if we write it as a condition for $T(\sigma)$:

$$\left(T(\sigma) - T(-\sigma) + 4\pi i\left(\lambda_l\delta'(\sigma) + \lambda_r\delta'(\sigma-\pi)\right)\right)|B\rangle^{\epsilon_b}_{\epsilon_l\epsilon_r} = 0. \qquad (2\cdot25)$$

Free bosons twisted by flux

One of the most straightforward generalizations of free boson OBS is the inclusion of the fluxes. In the case of a closed string, the boundary condition becomes (for example, see Ref. 4))

$$(\partial_{\bar{z}} X^\mu - \mathcal{O}^\mu_\nu \partial_z X^\nu) \, |B\rangle^{\mathcal{O}} = 0 \,, \quad \text{where } \mathcal{O} = (1 + F)(1 - F)^{-1} \,. \tag{2·26}$$

Here, $\mathcal{O}$ satisfies the orthogonality condition $\mathcal{O} \cdot \mathcal{O}^t = 1$ and is an element of O(d) (where d is the number of dimensions in which the flux $F_{\mu\nu}$ is introduced).

In order to define OBS, we have to specify three D-branes, which are located on the left, right and bottom. We consider the situation in which these D-branes have the fluxes F_l, F_r and F_b, and we denote the orthogonal matrices associated with these fluxes as $\mathcal{O}_l$, $\mathcal{O}_r$ and $\mathcal{O}_b$, respectively. The identifications of the holomorphic and anti-holomorphic oscillators at the three sides become

$$(\partial_{\bar{z}} X^\mu + (\mathcal{O}_l)^\mu_\nu \partial_z X^\nu)|_{\sigma=0} = 0 \,, \qquad (\partial_{\bar{z}} X^\mu + (\mathcal{O}_r)^\mu_\nu \partial_z X^\nu)|_{\sigma=\pi} = 0 \,, \tag{2·27}$$

$$(\partial_{\bar{z}} X^\mu - (\mathcal{O}_b)^\mu_\nu \partial_z X^\nu) \, |B^o\rangle^{\mathcal{O}_b}_{\mathcal{O}_l \mathcal{O}_r} = 0 \,. \tag{2·28}$$

The two conditions on the first line are used to determine the identification of the anti-holomorphic part with the holomorphic part and fix the periodicity of the latter under the shift $\sigma \to \sigma + 2\pi$. The condition on the second line represents the explicit definition of OBS in terms of holomorphic oscillators.

These constraints have the same form as those used in the general discussion if we make the replacements $\Sigma_b \to \mathcal{O}_b$, $\Lambda_r \to -\mathcal{O}_r$ and $\Lambda_l \to \mathcal{O}_l$, and hence we can use the consistency conditions derived there. In the present case they can be written as

$$\mathcal{O}_b^T \mathcal{O}_l = \mathcal{O}_l^T \mathcal{O}_b \,, \quad \mathcal{O}_b^T \mathcal{O}_r = \mathcal{O}_r^T \mathcal{O}_b \,. \tag{2·29}$$

We do not attempt to write explicitly all the matrices that solve these constraints. However, it is rather easy to see that there are many of solutions. A trivial solution is $\mathcal{O}_{b,l,r} = \epsilon_{b,l,r}\mathcal{O}$, where $\mathcal{O} \in$ O(d) and $\epsilon_{b,l,r} = \pm 1$. This gives a D-brane with the same flux or its T-dual.

For a more nontrivial solution, let us note that if we define $A = \mathcal{O}_r^T \mathcal{O}_b$, then we have $A \in$ O(d), and the constraint (2·29) implies $A^2 = 1$. This is not so difficult to solve for small values of d. The simplest nontrivial case is $d = 2$, for which there is a one-parameter family for A,

$$A = \mathcal{O}_r^T \mathcal{O}_b = \begin{pmatrix} \cos\theta & \sin\theta \\ \sin\theta & -\cos\theta \end{pmatrix} = \begin{pmatrix} \cos\theta_1 & -\sin\theta_1 \\ \sin\theta_1 & \cos\theta_1 \end{pmatrix} \begin{pmatrix} \cos\theta_1 & \sin\theta_2 \\ \sin\theta_2 & -\cos\theta_2 \end{pmatrix} \,, \tag{2·30}$$

with $\theta = \theta_1 + \theta_2$. This implies that there is a large class of solutions of the form

$$\mathcal{O}_r = \begin{pmatrix} \cos\theta_1 & -\sin\theta_1 \\ \sin\theta_1 & \cos\theta_1 \end{pmatrix} \,, \mathcal{O}_l = \begin{pmatrix} \cos\theta_2 & -\sin\theta_2 \\ \sin\theta_2 & \cos\theta_2 \end{pmatrix} \,,$$

$$\mathcal{O}_b = \begin{pmatrix} \cos\theta_3 & \sin\theta_3 \\ \sin\theta_3 & -\cos\theta_3 \end{pmatrix} \,, \tag{2·31}$$

for arbitrary $\theta_{1,2,3} \in \boldsymbol{R}$.

The interpretation of this solution is straightforward. Suppose we choose $\theta_3 = 0$. The $\mathcal{O}_b$ in this case describes a D1-brane in 2 dimensions. The angle θ_3 will rotate this D1-brane in an arbitrary direction. On the other hand, the D-branes on the left and right are D2-branes with arbitrary flux. We note that there are also solutions for which the left and right D-branes are D1 branes at arbitrary angles and the bottom one is a D2-brane with arbitrary flux.

Once the constraints (2·29) are solved, the mode expansion of X is determined so as to satisfy the periodicity condition

$$\partial X(\sigma + 2\pi) = \mathcal{O}_r^T \mathcal{O}_l \partial X(\sigma) , \tag{2·32}$$

and the boundary state is determined by the condition

$$(\partial X(-\sigma) + \mathcal{O}_l^T \mathcal{O}_b \partial X(\sigma))|B^o\rangle_{\mathcal{O}_l \mathcal{O}_r}^{\mathcal{O}_b} = 0 . \tag{2·33}$$

While these expressions are rather formal, it is not difficult to confirm that these definitions are consistent.

Ghosts

For the investigation of a bosonic string, we need the open boundary state for the reparametrization ghosts. Unlike the Majorana fermions, which turn out to be more nontrivial, the open boundary state for the ghost fields can be obtained in a straightforward manner. Here, the boundary conditions become,

$$(b_n - b_{-n})|B^o\rangle^{(\mathrm{gh})} = (c_n + c_{-n})|B^o\rangle^{(\mathrm{gh})} = 0 . \tag{2·34}$$

These conditions can be solved immediately as

$$|B^o\rangle^{(\mathrm{gh})} = \exp \left(\sum_{n>0} c_{-n} b_{-n} \right) c_0 c_1 |0\rangle^{(\mathrm{gh})} , \tag{2·35}$$

where $|0\rangle^{(\mathrm{gh})}$ is the $\mathrm{SL}(2, \boldsymbol{R})$-invariant ghost vacuum.

As mentioned above, the inner product between the open boundary states describes a rectangular worldsheet . At the corners, we have a deficit angle of $\pi/2$, which leads to some nontrivial features of the OBS. We give a systematic description for generic CFT in the next section. Here we give a short description which is specific to the ghost field. In this case, the effect of the deficit angle appears as the (implicit) ghost insertion at both ends of an open string. This can be seen in the following way. Let us focus on one of the two endpoints, say $\sigma = 0$:

$$c(u)|B^o\rangle^{(\mathrm{gh})} \sim \mathcal{O}(u), \quad b(u)|B^o\rangle^{(\mathrm{gh})} \sim \mathcal{O}(1). \tag{2·36}$$

The deficit angle at the corner is mapped to a smooth boundary by the conformal map $z = u^2$. In terms of this new coordinate z, we obtain the following behavior of the b and c fields in the upper half plane:

$$c(z) = 2u c(u) \propto z, \quad b(z) = (2u)^{-2} b(u) \propto \frac{1}{z}. \tag{2·37}$$

These relations imply that in the state (2·35), the ghost operator c has been inserted at $\sigma = 0$ in the smooth coordinate z. We interpret this as meaning that the corners are "marked points" on the worldsheet where ghost fields are inserted. They fix the symmetry associated with the conformal Killing vectors and reproduce the FP determinant. We will return to this point in §4.

BRST property of OBS

In string theory, a physical state condition is written in terms of a BRST operator. For the open string boundary state, it gives a nontrivial constraint, due to the anomaly at the corner (2·23). In bosonic string theory, the BRST operator in the general background can be written as

$$Q_B = \sum_{n \in \mathbf{Z}} c_n L_{-n}^{\mathrm{mat}} + \sum_{m,n \in \mathbf{Z}} \frac{m - n}{2} : c_m c_n b_{-m-n} : - c_0 , \qquad (2\cdot38)$$

and the open boundary state for free bosons takes the form

$$|B^o\rangle \equiv \prod_{\mathrm{bosons}} |B^o\rangle_{\epsilon_l \epsilon_r}^{\epsilon_b} \otimes |B^o\rangle^{(\mathrm{gh})} . \qquad (2\cdot39)$$

When we apply the BRST operator to this boundary state, the result is

$$
\begin{aligned}
Q_B |B^o\rangle &= -\sum_{n=1}^{\infty} c_{-n} \sum_{\mathrm{bosons}} (d_n)_{\epsilon_l \epsilon_r}^{\epsilon_b} |B^o\rangle - \sum_{n=1}^{\infty} 3n c_{-2n} |B^o\rangle \\
&= -\sum_{n=1}^{\infty} c_{-n} n \left[\left(\frac{1}{8} \sum_{\mathrm{bosons}} \epsilon_b \epsilon_l + \frac{3}{4} \right) + (-1)^n \left(\frac{1}{8} \sum_{\mathrm{bosons}} \epsilon_b \epsilon_r + \frac{3}{4} \right) \right] (2\cdot40)
\end{aligned}
$$

where we have used (2·23). Hence, the BRST invariance $Q_B|B^o\rangle = 0$ is equivalent to

$$\sum_{\mathrm{bosons}} \epsilon_b \epsilon_l = -6, \qquad \sum_{\mathrm{bosons}} \epsilon_b \epsilon_r = -6 . \qquad (2\cdot41)$$

For a more general background, we expect that the Virasoro condition for the OBS remains in same form (2·23), since it reflects the general behavior of the stress tensor at the corner as we see in the next section. In terms of this language, the above conditions are replaced by $\lambda_l = \lambda_r = 3/8$, where λ_l and λ_r are the conformal weights of the operators inserted at the corners. Usually, the operator that is inserted at the boundary should have a conformal weight 1 in order to maintain conformal invariance. We argue in the next section that this deviation comes from the anomaly associated with the deficit angle at the corner.

Modular covariance of rectangular diagram

We can check the consistency of these states by calculating their inner product and compare it with the usual path integral formula. This gives a disk amplitude in the form of a rectangle, whose sides are specified by various boundary conditions.

Although this is a disk diagram, we conjecture that the modular invariance (1·4) holds.

For the free case, we can readily confirm (1·4).[*] A straightforward computation gives

$$I_{(\epsilon_t|\epsilon_l,\epsilon_r|\epsilon_b)}(t) \equiv {}^{\epsilon_t}_{\epsilon_r\epsilon_l}\langle B|q^{L_0^{\epsilon_l\epsilon_r}+a^{\epsilon_l\epsilon_r}}|B\rangle^{\epsilon_b}_{\epsilon_l\epsilon_r} = \frac{q^{a^{\epsilon_l\epsilon_r}}}{\prod_{n>0}\sqrt{1-\epsilon_t\epsilon_b q^{2n}}}I^{(\text{zero})}_{(\epsilon_t|\epsilon_l,\epsilon_r|\epsilon_b)}(t)\,, \quad (2\cdot42)$$

where $q = e^{-\pi t}$, and the zero-point energy $a^{\epsilon_l\epsilon_r}$ is given by

$$a^{\epsilon_l\epsilon_r} = -\frac{1}{24} \quad \text{for } \epsilon_l\epsilon_r = +1, \quad a^{\epsilon_l\epsilon_r} = \frac{1}{48} \quad \text{for } \epsilon_l\epsilon_r = -1. \quad (2\cdot43)$$

As in the previous case, n in (2·42) runs over positive integers for $\epsilon_l\epsilon_r = 1$ and positive half odd integers for $\epsilon_l\epsilon_r = -1$. We denote the contribution of the zero mode as $I^{(\text{zero})}_{(\epsilon_t|\epsilon_l,\epsilon_r|\epsilon_b)}$. It is nontrivial when $\epsilon_l = \epsilon_r = +1$ (NN) and trivial (i.e. $I^{(\text{zero})}_{(\epsilon_t|\epsilon_l,\epsilon_r|\epsilon_b)} = 1$) in all other cases, because unless $\epsilon_l = \epsilon_r = +1$, (ϵ_l, ϵ_r)-strings have no zero modes. There are four cases corresponding to the former condition, $\epsilon_l = \epsilon_r = +1$, but only one of them gives a nontrivial contribution,

$$I^{(\text{zero})}_{(D|N,N|D)} = \frac{1}{\sqrt{\alpha't}}, \quad I^{(\text{zero})}_{(N|N,N|N)} = I^{(\text{zero})}_{(N|N,N|D)} = I^{(\text{zero})}_{(D|N,N|N)} = 1. \quad (2\cdot44)$$

Here we have used the following zero mode conventions:[**]

$$\widehat{x} = \frac{i}{2}(\widehat{a} - \widehat{a}^\dagger), \ \widehat{p} = \widehat{a} + \widehat{a}^\dagger, \ [\widehat{a}, \widehat{a}^\dagger] = 1$$

$$|x_0\rangle = \left(\frac{2}{\pi}\right)^{\frac{1}{4}}e^{\frac{1}{2}\widehat{a}^{\dagger 2}-2ix_0\widehat{a}^\dagger-x_0^2}|0\rangle, \ |p_0\rangle = (2\pi)^{\frac{1}{4}}e^{-\frac{1}{2}\widehat{a}^{\dagger 2}+p_0\widehat{a}^\dagger-\frac{1}{4}p_0^2}|0\rangle \quad (2\cdot46)$$

$$\widehat{p}|p_0\rangle = p_0|p_0\rangle, \ \widehat{x}|x_0\rangle = x_0|x_0\rangle$$

Including these zero mode contributions, we obtain the following expression for the rectangle amplitude for a free boson:

$$I_{(N|N,N|N)} = I_{(D|D,D|D)} = I_{(N|D,D|N)} = \frac{1}{\eta^{1/2}(t)}, \quad (2\cdot47)$$

$$I_{(D|N,N|D)} = \frac{1}{(\alpha't)^{1/2}\eta^{1/2}(t)}, \quad I_{(D|N,N|N)} = I_{(D|D,D|N)} = \frac{\eta^{1/2}(t)}{\eta^{1/2}(2t)}, \quad (2\cdot48)$$

$$I_{(N|N,D|N)} = I_{(D|N,D|D)} = \frac{\eta^{1/2}(t)}{\eta^{1/2}(t/2)}, \quad I_{(N|N,D|D)} = \frac{\eta^{1/2}(2t)\eta^{1/2}(t/2)}{\eta(t)}. \quad (2\cdot49)$$

---

[*] A useful formula is

$$\langle 0|e^{qa^2/2}e^{\pm(a^\dagger)^2/2}|0\rangle = (1-q)^{\mp 1/2}$$

for a simple oscillator, with $[a, a^\dagger] = 1$.

[**] We note that in deriving $I^{(\text{zero})}_{(D|N,N|D)} = \frac{1}{\sqrt{\alpha't}}$, we set the position eigenvalues of the zero mode all equal, with the value x_0. If they are not all equal, we have to replace $I^{(\text{zero})}_{(D|N,N|D)}$ by

$$\langle x_0|q^{\alpha'\widehat{p}^2}|y_0\rangle = \left(-\frac{\pi}{\alpha'\ln q}\right)^{\frac{1}{2}}\exp\left(\frac{(x_0-y_0)^2}{\alpha'\ln q}\right). \quad (2\cdot45)$$

As a consistency check, we study the modular property of these partition functions. We can write this property as

$$I_{(\epsilon_1|\epsilon_2,\epsilon_4|\epsilon_3)}(1/t) = t^w I_{(\epsilon_4|\epsilon_1,\epsilon_3|\epsilon_2)}(t) \, , \tag{2.50}$$

where w is some weight which may depend on the boundary conditions. By using the explicit forms given above, we can confirm this relation with the weight

$$w = -\frac{1}{16}(\epsilon_1\epsilon_2 + \epsilon_2\epsilon_3 + \epsilon_3\epsilon_4 + \epsilon_4\epsilon_1) \, . \tag{2.51}$$

These factors have a structure similar to that of the coefficients of the anomaly term in (2.25). In the next section, we see that they are indeed closely related.

We can make a similar calculation for the ghost sector. The rectangle amplitude for the ghost field is

$$I_{\text{ghost}}(t) = {}^{\text{(gh)}}\langle B^o|b_0 q^{L_0^{\text{(gh)}}+\frac{1}{12}}|B^0\rangle^{\text{(gh)}} = \eta(t), \tag{2.52}$$

and its modular property is

$$I_{\text{ghost}}(1/t) = t^{1/2} I_{\text{ghost}}(t) \, . \tag{2.53}$$

This is the square root of the contribution of the ghost boundary state in the closed string.

A consistency condition for a bosonic string

Let us consider a bosonic string theory with flat intersecting D-branes. In this case, the rectangle amplitude can be written as the product $I^{\text{tot}} = I_{\text{ghost}}\prod_{\text{bosons}} I$, where $\prod_{\text{bosons}}$ represents the product over 26 boson fields. From (2.50) and (2.53), the modular property of I^{tot} is

$$I^{\text{tot}}(1/t) = t^{w_{\text{tot}}} I^{\text{tot}}(t) \, , \tag{2.54}$$

where the total weight w_{tot} is given by

$$w_{\text{tot}} = -\frac{1}{16}\sum_{\text{bosons}}\sum_{i=1}^{4}\epsilon_i\epsilon_{i+1} + \frac{1}{2} \, . \tag{2.55}$$

The rectangle amplitude describes the propagation of an open string between the two D-branes Σ_b and Σ_t,

$$A = \int_0^\infty I^{\text{tot}}_{(\Sigma_t|\Lambda_l,\Lambda_r|\Sigma_b)}(t)dt \, . \tag{2.56}$$

This amplitude can also be interpreted as the propagation from Λ_l and Λ_r in the modular dual channel, and A should be invariant. This implies that the total weight w_{tot} must be 2. Actually, we can show that this is the case if the BRST constraint (2.41) is satisfied.

§3. CFT at the corner

In §2 we computed rectangle amplitudes with various boundary conditions, and found that they are transformed under modular transformations as modular forms. The factor t^w on the right-hand side of (2·50) can be interpreted as a conformal factor arising in the dilatation of the rectangular worldsheet from the size $1 \times t$ to $1/t \times 1$. With this interpretation, each term $-\epsilon_i\epsilon_{i+1}/16$ in the modular weight (2·51) seems to be the conformal weight associated with each corner of the rectangle. In this section, we first derive the basic properties of CFT near the corner, with special attention given to the change of the conformal weight of the primary fields.[*] We then prove that, for the rectangular diagram, the conformal weight at each corner indeed gives the modular weight of the modular transformation of the rectangular diagram.

CFT at the corner

Let us focus on the vicinity of one corner and use the first quadrant instead of a rectangle. The map between the upper half plane with the coordinate z' and the first quadrant with the coordinate z is given by $z' = z^2$. In the following, we study the slightly more general case of $z' = z^n$.

Let $\mathcal{O}$ be a primary operator with conformal weight λ. We insert this operator at the origin of the z'-plane. Then, at the origin, the energy momentum tensor $T(z')$ has the double pole singularity

$$T(z') = \frac{\lambda}{z'^2} + \cdots , \tag{3·1}$$

where the dots represent a simple pole and the finite part. For a general conformal map of the form $z' = f(z)$, the energy momentum tensor in a theory with central charge c is transformed according to

$$T(z) = (f')^2 T(z') + c\left(\frac{f'''}{12f'} - \frac{(f'')^2}{8(f')^2} \right). \tag{3·2}$$

Using this formula for the conformal map $z' = z^n$, we can translate the behavior of $T(z')$ in (3·1) to the following behavior of $T(z)$ near the corner:

$$T(z) = \left(n^2\lambda - c\frac{n^2 - 1}{24} \right)\frac{1}{z^2} + \cdots . \tag{3·3}$$

In order to evaluate the conformal weight associated with the corner, we have to divide the coefficient of $1/z^2$ by n:[**]

$$\lambda_{\text{corner}} = n\lambda - c\frac{n^2 - 1}{24n}. \tag{3·4}$$

---

[*] For related studies of CFT at the corner, see, for example, Refs. 14) and 15).

[**] This factor appears because the dilatation operator near the edge is given by the integral of $T(z)$ over the contour consisting of $1/n$ of the usual half-circle. More explicitly, this integral is taken over the path $z = re^{i\theta}$ with $0 \leq \theta \leq \pi/n$.

The first term on the right-hand side of this relation represents the contribution of the inserted operator, and the second term is the intrinsic weight of the corner.

When boundary conditions on both sides of the corner are the same (i.e.,DD or NN), we need no operator insertion at the origin of z', and we have $\lambda = 0$. In this case the equality $\lambda_{\text{corner}} = -1/16$ holds for each free boson. By contrast, if the two boundary conditions are different (ND or DN), we need to insert the twist operator σ for the boson field. In this case, because σ has conformal weight $1/16$, Eq.(3·4) gives $\lambda_{\text{corner}} = +1/16$. These results can be combined to give $\lambda_{\text{corner}} = -\epsilon_i \epsilon_{i+1}/16$, which coincides with the modular weight of the rectangle at one corner. At the same time, it accounts for the anomaly at the corners in (2·25), if we note

$$\text{disc}\frac{1}{z^2} = -2\pi i\delta'(\sigma)\,. \tag{3·5}$$

The change of the conformal weight of the primary fields can be interpreted as the renormalization effect induced by the conformal map. We now rederive the first term in (3·4), that is, the contribution of the inserted operator. Let us consider the conformal map $z' = z^n$ again. Because the corner is a singular point, we have to be careful when we insert an operator there. To see what kind of singularity arises, we first insert the operator at a generic point z, and then take the limit $z \to 0$. The primary fields $\mathcal{O}(z)$ and $\mathcal{O}(z')$ are related as

$$\mathcal{O}(z' = 0) = \lim_{z \to 0}(nz^{n-1})^\lambda \mathcal{O}(z). \tag{3·6}$$

Because the z'-plane is smooth, the insertion of $\mathcal{O}(z')$ does not produce any singularity in the $z' \to 0$ limit. This fact and the relation (3·6) together imply that the operator $\mathcal{O}(z)$ in the z-plane behaves as $\sim (nz^{n-1})^\lambda$. Therefore, in order to have a well-defined vertex insertion, we should use the renormalized operator

$$\mathcal{O}^{\text{ren}}(z) = \frac{1}{(nz^{n-1})^\lambda}\mathcal{O}(z). \tag{3·7}$$

The renormalization factor gives an extra contribution to the conformal weight. The factor $(nz^{n-1})^{-\lambda}$ has conformal weight $(n-1)\lambda$, and the total conformal weight of the renormalized operator is $n\lambda$. This is what we have in (3·4).

Multiplication of tachyon vertices with OBS

As a simple example, let us consider an OBS with tachyon vertices inserted at the corners. The (bare) tachyon vertex is

$$V_k(z) =: e^{-ikX(z)} : . \tag{3·8}$$

The conformal weight of this operator is $\lambda = \alpha'k^2$.

We can explicitly see the singular behavior of this operator near the corner $\sigma = 0$ if we apply this operator to the OBS. This is done below. We use NNN boundary conditions for concreteness. First, Wick's theorem gives

$$V(0,\tau)|B^o\rangle_{NN}^N = e^{-ik\hat{x}} \prod_{n=1}^{\infty} \exp\left(-2\sqrt{2\alpha'}k\frac{a_{-n}}{2n}e^{n\tau}\right) \exp\left(2\sqrt{2\alpha'}k\frac{a_n}{2n}e^{-n\tau}\right) |B^o\rangle_{NN}^N$$

$$= (1 - e^{-2\tau})^{\alpha' k^2} e^{-ik\widehat{x}} \prod_{n=1}^{\infty} \exp\left(-2\sqrt{2\alpha'}k\frac{a_{-n}}{n}\cosh(n\tau)\right) |B^o\rangle_{NN}^N$$

$$\sim (2\tau)^{\alpha' k^2} e^{-ik\widehat{x}} \prod_{n=1}^{\infty} \exp\left(-2\sqrt{2\alpha'}k\frac{a_{-n}}{n}\right) |B^o\rangle_{NN}^N . \tag{3.9}$$

Because of the factor $(2\tau)^{\alpha' k^2}$, this is singular at $\tau = 0$. An operator inserted near the other corner, $\sigma = \pi$, produces a similar singularity. In order to remove this singularity, we define the following renormalized vertex operator:

$$V_k^{\mathrm{ren}}(\tau, \sigma) = (2\tau)^{-\alpha' k^2} V_k(\tau, \sigma). \tag{3.10}$$

This kind of renormalization is familiar in the relation between the bulk operator and the boundary operator. For example, a bulk operator $e^{ik\phi}$ has conformal weight $(\alpha' k^2/2, \alpha' k^2/2)$. Therefore, we could naively expect the conformal weight $\alpha' k^2/2 + \alpha' k^2/2 = \alpha' k^2$ for a boundary operator of the same form. However, the actual value is $2\alpha' k^2$. This is because the limit in which the operator approaches the boundary is singular, and therefore we need an extra renormalization factor, which doubles the conformal weight.

Localization of the weight at the corners

Finally, we can show the localization of the weight at the corners for the rectangle amplitude in the following way. Let us consider a rectangular worldsheet, and let a and b denote the lengths along the τ and σ directions, respectively. The deformation of the worldsheet is generated by the energy momentum tensor. For example, a change of the length b to $b+\delta b$ is generated by $\delta b L_0 = \delta b \int_{C_2} \frac{d\sigma}{2\pi} T +$ [anti-holomorphic part], where the contour C_2 is a segment crossing worldsheet from one boundary, $\sigma = 0$, to the opposite boundary, $\sigma = a$. Similarly, the change of the length a is generated by the insertion of T along the contour C_1, which goes from the boundary $\tau = 0$ to $\tau = b$. Combining these two, we can generate the dilatation of the worldsheet, and the change of amplitude resulting from the dilatation is given by

$$\frac{\delta I}{I} = \left\langle \oint_{C_1} \frac{dz}{2\pi i} aT + \oint_{C_2} \frac{dz}{2\pi i} ibT \right\rangle + \text{c.c.} \tag{3.11}$$

where c.c. (complex conjugate) represents the contribution of the anti-holomorphic part [see Fig.2 (a)]. We can deform the two contours into four contours going around each corner. Doing so, we rewrite (3.11) as

$$\frac{\delta I}{I} = \sum_{i=1}^{4} \left\langle \oint_{z_i} \frac{dz}{2\pi i} (z - z_i)T \right\rangle + \text{c.c.}, \tag{3.12}$$

where z_i $(i = 1, 2, 3, 4)$ are the coordinates of the four corners, and $\int_{z_i}$ represents integration along the contour around z_i [see Fig.2 (b)]. In (3.12), the integral for each i extracts the conformal weight of the i-th corner. This argument implies that the effect of the dilatation is obtained by summing the conformal weights associated with the corners.
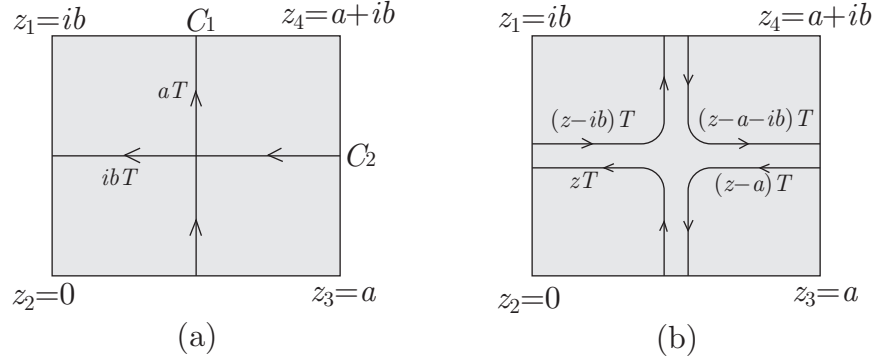
Fig. 2. (a) The dilatation is generated by the energy momentum tensor inserted along the two contours C_1 and C_2. The operators integrated along each contour are shown beside that contour. (b) The two contours in (a) can be rearranged into four contours around each corner. The integral along each contour gives the conformal weight of the corresponding corner. In both (a) and (b), we show only the holomorphic parts.

§4. Path integral approach to the rectangle amplitude

In this section, we present the path integral evaluation of the rectangle amplitude and confirm that it is identical to the results obtained from OBS.

4.1. *Direct evaluation of the path integral*

Formally, the amplitude is obtained from the Gaussian integral

$$I = \int \mathcal{D}X e^{-S[X]} = (\det \Delta)^{-1/2}, \tag{4.1}$$

where $S[X]$ is the action of the matter part,

$$S[X] = \frac{1}{4\pi\alpha'} \int d^2\sigma X \Delta X \tag{4.2}$$

and Δ is (up to a sign) the Laplacian on the worldsheet,

$$\Delta = -\frac{\partial^2}{\partial\tau^2} - \frac{\partial^2}{\partial\sigma^2}. \tag{4.3}$$

In this section, we assume that all the boundary conditions are Dirichlet for simplicity. Other boundary conditions can be treated similarly.

First, let us rederive the rectangle amplitude $I_{(D|D,D|D)}$ in (2·47) with the path integral approach. If the worldsheet is a rectangle of size $a \times b$, then X has the mode expansion

$$X(\sigma,\tau) = \sum_{m,n\geq 1} X_{mn} \sin\left(\frac{m\pi\tau}{a}\right) \sin\left(\frac{n\pi\sigma}{b}\right). \tag{4.4}$$

The eigenvalues of the operator Δ for the eigenfunctions in (4·4) are

$$\lambda_{m,n} = \frac{\pi^2 m^2}{a^2} + \frac{\pi^2 n^2}{b^2}, \quad m,n = 1,2,\ldots. \tag{4.5}$$

Then, the determinant of the operator Δ is represented by the infinite product of all the eigenvalues

$$I = (\det \Delta)^{-1/2} = \prod_{m,n=1}^{\infty} \lambda_{m,n}^{-1/2}. \tag{4·6}$$

An advantage of the path integral approach is that the modular invariance is manifest by definition. Indeed, the amplitude (4·6) is invariant under the exchange of a and b. However, this property has only a formal significance unless we regularize this divergent product of the eigenvalues.

A simple way to obtain a finite result is to use the ζ-function regularization. In this method, we first rewrite (4·6) as

$$I = \prod_{m,n \geq 1} \lambda_{m,n}^{-1/2} = \prod_{m,n \geq 1} \frac{b}{\pi n} \left(1 + \frac{m^2 t^2}{n^2}\right)^{-1/2}, \tag{4·7}$$

where $t = b/a$. Let us carry out the product with respect to n. Removing the divergent constant factor $\prod_{n=1}^{\infty}(1/\pi n)$ independent of a and b, and using the formula $\prod_{n=1}^{\infty}(1 + x^2/n^2) = \sinh \pi x/(\pi x)$ for the convergent product and the ζ-function regularization formulae $\prod_{n=1}^{\infty} x = x^{\zeta(0)} = x^{-1/2}$ and $\prod_{m=1}^{\infty} q^m = q^{\zeta(-1)} = q^{-1/12}$, we obtain

$$I \propto \prod_{m=1}^{\infty} b^{-1/2} \left(\frac{\sinh \pi m t}{\pi m t}\right)^{-1/2} = \prod_{m=1}^{\infty} \left(\frac{a q^{-m}}{2\pi m}(1 - q^{-2m})\right)^{-1/2} \propto ((ab)^{-1/4} t^{1/4} \eta(t))^{-1/2}, \tag{4·8}$$

where $q = e^{-\pi t}$. The t-dependent part of this amplitude coincides with the amplitude we obtained using the oscillator approach, and the area dependence reproduces the correct conformal weight, $-1/4$.

Although the ζ-function regularization provides a simple and efficient way to extract a finite result from the divergent product, its physical meaning is unclear. For this reason, we give another derivation of the same result using a more conventional regularization method, the heat kernel method, in which we introduce a cut-off ϵ and regularize the determinant by writing

$$\Gamma = \log \det \Delta = -\int_{\epsilon}^{\infty} \frac{d\xi}{\xi} \operatorname{tr} e^{-\xi \Delta}, \tag{4·9}$$

where we have defined Γ through the relation $I = e^{-\Gamma/2}$. Then, for the rectangle with eigenvalues (4·5), we obtain

$$\Gamma = -\int_{\epsilon}^{\infty} \frac{d\xi}{\xi} \sum_{m,n} e^{-\xi \lambda_{m,n}} = -\frac{1}{4} \int_{\epsilon}^{\infty} \frac{d\xi}{\xi} \left(\theta_3\left(\frac{\pi\xi}{a^2}\right) - 1\right) \left(\theta_3\left(\frac{\pi\xi}{b^2}\right) - 1\right)$$

$$= -\frac{ab}{4\pi\epsilon} + \frac{2(a+b)}{4\sqrt{\pi\epsilon}} - \frac{1}{4} \log \frac{ab}{\pi\epsilon} + \log(t^{1/4}\eta(t)) + \frac{\gamma - \log 4\pi}{4} + \mathcal{O}(\epsilon). \tag{4·10}$$

The first two terms here are cancelled by local counterterms and have no physical meaning. The remaining part correctly reproduces the previous result (4·8), up to a constant.

4.2. *Derivation of the rectangular diagram from the Weyl anomaly*

For a general worldsheet with boundaries, a formula for the determinant defined with the regularization (4·9) is given in Ref. 17). This gives the determinant as an anomaly associated with the Weyl rescaling $g_{ab} = e^{2\sigma}\widehat{g}_{ab}$, where $\widehat{g}_{ab}$ is a fiducial reference metric. Specifically, it gives the determinant as a functional of σ:

$$\log I = -\frac{1}{2}(\varGamma_{\mathrm{div}} + \varGamma_{\mathrm{bulk}} + \varGamma_{\mathrm{bdr}} + \cdots),$$

$$\varGamma_{\mathrm{div}} = -\frac{1}{4\pi\epsilon}\int d^2z\sqrt{\widehat{g}}e^{2\sigma} + \frac{1}{4\sqrt{\pi\epsilon}}\int d\widehat{s}e^{\sigma} + \frac{1}{6}\chi(M)\log\epsilon,$$

$$\varGamma_{\mathrm{bulk}} = -\frac{1}{12\pi}\int_M \sqrt{\widehat{g}}\widehat{g}^{ab}(\partial_a\sigma)(\partial_b\sigma),$$

$$\varGamma_{\mathrm{bdr}} = -\frac{1}{6\pi}\left(\int_{\partial M}d\widehat{s}\widehat{k}\sigma + \frac{1}{2}\int_M d^2z\sqrt{\widehat{g}}\widehat{R}\sigma\right). \tag{4·11}$$

Here, $\varGamma_{\mathrm{div}}$ represents the divergent part depending on the cutoff ϵ, and $\varGamma_{\mathrm{bulk}}$ and $\varGamma_{\mathrm{bdr}}$ are finite contributions from the bulk and the boundary of the worldsheet, respectively. (Although $\varGamma_{\mathrm{bdr}}$ includes the bulk integral term, it vanishes in the computation carried out below.) The dots represent terms independent of σ, in which we are not interested. The first two terms in $\varGamma_{\mathrm{div}}$ are divergent terms proportional to the area of the worldsheet and the length of the boundary, respectively. They are invariant under the renormalization flow in the sense that a rescaling of the cutoff, $\epsilon \to e^{2\alpha}\epsilon$, is absorbed by the constant shift $\sigma \to \sigma + \alpha$. The third term in $\varGamma_{\mathrm{div}}$, which is logarithmically divergent, is also invariant under renormalization if it is combined with $\varGamma_{\mathrm{bdr}}$. The rescaling of the cutoff changes the third term of $\varGamma_{\mathrm{div}}$ by $(\alpha/3)\chi(M)$, and this is cancelled by the change of $\varGamma_{\mathrm{bdr}}$ under the constant shift $\sigma \to \sigma + \alpha$,

$$\delta\varGamma_{\mathrm{bdr}} = -\frac{\alpha}{6\pi}\left(\int_{\partial M}d\widehat{s}\widehat{k} + \frac{1}{2}\int_M d^2z\sqrt{\widehat{g}}\widehat{R}\right) = -\frac{\alpha}{3}\chi(M). \tag{4·12}$$

In this way, logarithmically divergent terms are always accompanied by finite terms which make the overall amplitude renormalization invariant. Using this fact, we can determine the scale dependence of amplitudes from their cutoff dependence.

For a rectangle of size $a \times b$, the first two terms in $\varGamma_{\mathrm{div}}$ are identical to the first two terms in (4·10). However, the logarithmically divergent term, which is related to the conformal weight of the amplitudes, does not coincide with the corresponding term in (4·10). As we see from (4·12), the formula (4·11) gives a conformal weight $-1/6$ for any amplitude in the case of disk topology, while we know that the rectangle amplitudes have the conformal weight $-1/4$. In order to resolve this problem, we have to treat the divergence of the integral at the corners more carefully.

In order to see how the divergence at each corner modifies the conformal weight, let us focus on one of corners. We consider slightly generalized situation in which the corner has an angle of π/n. We can always choose coordinates z and u for which the mapping around the corner is represented by $z \propto u^n$. We employ the flat metric on the z-plane as the reference metric $\widehat{g}$, and g is the flat metric on the u-plane.

From (4·12), we can extract the conformal weight

$$\lambda(\text{boundary contribution}) = -\frac{n-1}{12n} \tag{4·13}$$

for the corner. As mentioned above, this part is not sufficient to reproduce the conformal weight of the corners. For this purpose, we also need to take account of the contribution of Γ_{bulk}. For the mapping $z \propto u^n$, it is given by

$$\Gamma_{\text{bulk}} = -\frac{1}{12\pi}\left(\frac{n-1}{n}\right)^2 \int d^2z \frac{1}{|z|^2}. \tag{4·14}$$

This integral diverges logarithmically in the limit $|z| \to 0$. (Note that the divergence in the limit $z \to \infty$ is of no concern here. Here we are focusing on the divergence at the corner.) In order to regularize this divergence, we introduce a small cutoff ρ, remove a sector of radius ρ from the corner, and integrate over only the region in the z-plane mapped to values of u satisfying $|u| \geq \rho$. We then have

$$\Gamma_{\text{bulk}} = \frac{(n-1)^2}{12n}\log\rho + (\rho \text{ independent part}). \tag{4·15}$$

This cutoff dependence gives a new contribution to the weight,

$$\lambda(\text{bulk contribution}) = -\frac{(n-1)^2}{24n}. \tag{4·16}$$

Adding (4·13) and (4·16), we obtain the correct value appearing in (3·4).

We can reproduce not only the conformal weight of a corner but also the full rectangle amplitude as a Weyl anomaly. For example, we can obtain a rectangle of arbitrary size $a \times b$ from a round disk of diameter d. Because the conformal map is singular at the corners of the rectangle and the bulk integral term diverges there, we remove small sectors around each corner. Let ρ_i $(i = 1, 2, 3, 4)$ denote the radii of the sectors defined with the metric on the rectangle. Then we obtain the following conformal anomaly associated with the conformal map:

$$\Gamma = \log t^{1/4}\eta(t) - \frac{1}{4}\log(ab) + \frac{1}{3}\log d - \frac{1}{6}\log 2 + \frac{1}{2}\log \pi + \frac{1}{24}\sum_{i=1}^{4}\log\rho_i. \tag{4·17}$$

Up to constant terms, this coincides with the rectangle amplitude we have obtained with other methods. Note that the dependence of (4·17) on each cutoff is the same as that of (4·15).

The important point here is that when the worldsheet with a corner is mapped to a worldsheet with a smooth boundary, the image of a corner is 'marked', because we need to regularize the bulk term by, for example, removing a small sector around each corner. Mapping a rectangle to a round disk, we obtain a disk with four marked points.

For this reason, the disk does not have conformal Killing vectors, and it has a single modulus t. When we compute the string amplitude, we have to insert a ghost operator at the four marked points, and we have to carry out a modulus integration accompanied by a b-field insertion.

§5.   Correlation functions

In the previous sections, we have established the open boundary state by demonstrating that it is identical to that derived with the path integral computation. There, we learned that a special care is needed in the treatment of the corner, especially when the vertex operator is inserted. In this section, we present some examples of the computation of the correlation functions in which tachyon vertex operators are inserted at the corners. These examples illuminate the prescriptions we have proposed.

OBS with tachyon insertions

We first consider the computation using OBS. By analyzing the modular properties of the correlation function, we reproduce the intrinsic weight of a corner of a rectangle and the renormalized conformal weight of the tachyon vertex operator at a corner discussed at the end of §3. First, we consider a single free boson X (i.e. the case $c = 1$) for simplicity. Since the zero mode exists only in the mode expansion of NN string, tachyon vertices can be inserted only at the corners located between two edges with Neumann boundary conditions. In order to evaluate amplitudes, we must define the OBS with two tachyon vertices inserted and one with one tachyon vertex inserted. The definition of the OBS with two tachyon vertices is expressed in terms of the renormalized tachyon vertex operators given in (3·10):

$$|B^o; k_1, k_2\rangle^N_{NN} \equiv \lim_{\tau_1, \tau_2 \to 0} V^{\mathrm{ren}}_{k_1}(\tau_1, 0) V^{\mathrm{ren}}_{k_2}(\tau_2, \pi) |B^o\rangle^N_{NN}$$

$$= 2^{\frac{\widetilde{k}_1 \widetilde{k}_2}{2}} e^{-i(k_1+k_2)\widehat{x}} \prod_{m=1}^{\infty} \exp\left(-\frac{\widetilde{k}_1 + (-)^m \widetilde{k}_2}{m} a_{-m}\right) |B^o\rangle^N_{NN}. \quad (5·1)$$

The definition of the OBS with one tachyon vertex is similar to that in the two vertex case considered above:

$$|B^o; k\rangle^N_{ND} \equiv \lim_{\tau \to 0} V^{\mathrm{ren}}_k(\tau, 0) |B^o\rangle^N_{ND} = e^{-ik\widehat{x}} \prod_{r=1/2}^{\infty} \exp\left(-\frac{\widetilde{k}}{r} a_{-r}\right) |B^o\rangle^N_{ND}. \quad (5·2)$$

Here we have defined the dimensionless momentum $\widetilde{k} \equiv 2\sqrt{2\alpha'}k$. Using $\widetilde{k}$, the on-shell momentum for a tachyon is $\widetilde{k}^2 = 8$.

Four tachyon insertions

When four edges of the rectangle have Neumann boundary conditions, we can insert tachyon vertices at all the corners (see Fig.3):

$$I_4(k_1, k_2; k_3, k_4; t) = {}^N_{NN}\langle B^o; k_3, k_4| q^{L^{NN}_0 - \frac{1}{24}} |B^o; k_1, k_2\rangle^N_{NN}$$

$$= 2^{\frac{\widetilde{12}+\widetilde{34}}{2}} \eta(t)^{\frac{1}{2}(\widetilde{1}^2+\widetilde{2}^2+\widetilde{3}^2+\widetilde{4}^2)-\frac{1}{2}} \left(\frac{\eta(t/2)}{\eta(t)}\right)^{(\widetilde{1}-\widetilde{2})(\widetilde{3}-\widetilde{4})} \left(\frac{\eta(2t)}{\eta(t)}\right)^{(\widetilde{1}-\widetilde{3})(\widetilde{2}-\widetilde{4})}. \quad (5·3)$$

(Henceforth we often use the notation $\widetilde{i} \equiv \widetilde{k}_i$.) Using a computation similar to that

Fig. 3. Rectangle amplitudes with tachyon vertex operators, specified by the momenta k_i.

Fig. 4. Modular properties of rectangle amplitudes with tachyon vertices

yielding (2·50), the modular property of this amplitude is obtained as

$$I_4\left(k_1, k_2; k_3, k_4; \frac{1}{t}\right) = t^{\frac{1}{4}(\tilde{1}^2+\tilde{2}^2+\tilde{3}^2+\tilde{4}^2-1)} I_4(k_1, k_3; k_2, k_4; t). \qquad (5\cdot4)$$

This property is graphically depicted in Fig.4 (a).

The factor $t^{\frac{1}{4}(\tilde{1}^2+\tilde{2}^2+\tilde{3}^2+\tilde{4}^2-1)}$ on the right-hand side shows that the conformal weight of the entire amplitude is $\frac{1}{4}(\tilde{1}^2 + \tilde{2}^2 + \tilde{3}^2 + \tilde{4}^2 - 1)$. This implies that the conformal weight of each tachyon vertex operator at a corner of the rectangle is $\tilde{k}^2/4 = 2\alpha'k^2$. This is identical to the weight of the *renormalized* vertex operator at the corner, discussed at the end of §3. This result comes from the use of the OBS with renormalized vertex operators. The factor $-1/4$ comes from the intrinsic weight of the corner (2·51), where all edges satisfy Neumann conditions.

We now comment on the relation between the on-shell condition of the tachyon vertex and the modular weight. The condition of modular invariance must be imposed on the total amplitude $I_{\text{tot}} = I_{\text{ghost}} \prod I_{\text{matter}}$. Here the index of the product runs over all spacetime dimensions, and I_{ghost} is the same as that used above. Hence, the total conformal weight w_{tot} is

$$w_{\text{tot}} = \frac{1}{4}(\tilde{1}^2 + \tilde{2}^2 + \tilde{3}^2 + \tilde{4}^2 - 26) + \frac{1}{2}. \qquad (5\cdot5)$$

In order for the amplitude $A = \int_0^\infty I_{\text{tot}}(t)\,dt$ to be modular invariant, w_{tot} must be equal to 2. If all the tachyons are on-shell, the conformal weight of the tachyon vertex

is $\widetilde{k}^2/8 = 1$, and therefore w_{tot} is in fact equal to 2. This implies the equivalence of the on-shell condition for the tachyon vertex and the modular invariance of the rectangle amplitude.

Comparison with UHP amplitude

We now give a different type of calculation of the amplitude using a conformal map and confirm the consistency with the results obtained in the previous subsection. This equivalence of these two approaches seems rather nontrivial.

The four tachyon amplitude $I_4^{\text{rec}}(k_i; t)$ is obtained by combining the ghost amplitude I_{ghost} in (2·52) and the amplitudes in (5·3) for 26 bosons as

$$I_4^{\text{rec}}(k_i; t) = 2^{2(s-4)} \eta(t)^4 \left(\frac{\eta(t/2)}{\eta(t)} \right)^{4(t-u)} \left(\frac{\eta(2t)}{\eta(t)} \right)^{4(s-u)}, \tag{5·6}$$

where we have assumed the on-shell condition $k_i^2 = 1/\alpha'$ and defined the Mandelstam variables $s = 2\alpha'(k_1 + k_2)^2$, $t = 2\alpha'(k_1 + k_3)^2$, and $u = 2\alpha'(k_2 + k_3)^2$.

Then, note that the same amplitude can be obtained as the correlation function in the upper half plane as

$$I_4^{\text{UHP}} = \langle ce^{-ik_3 X}(0) e^{-ik_1 X}(B) ce^{-ik_2 X}(1) ce^{-ik_4 X}(\infty) \rangle = (1 - B)^{s/2-2} B^{t/2-2}. \tag{5·7}$$

The next task is to determine the relation between the modulus t of the rectangle worldsheet and the cross ratio B of the 4-point function. The modulus t is defined by

$$it = \int_B^0 \frac{dx}{y} \bigg/ \int_B^1 \frac{dx}{y}, \quad y^2 = x(x-1)(x-B). \tag{5·8}$$

We can solve (5·8) to obtain B in terms of t. Then, we find that B and its derivative are given by

$$B = \frac{\eta^{16}(t/2)\eta^8(2t)}{\eta^{24}(t)}, \quad \frac{dB}{dt} = 16\pi \frac{\eta^{16}(t/2)\eta^{16}(2t)}{\eta^{28}(t)}. \tag{5·9}$$

Using these relations, we obtain

$$I_4^{\text{UHP}} dB = 16\pi I_4^{\text{rec}} dt. \tag{5·10}$$

Two tachyon insertions

When there are three edges with Neumann boundary conditions and an edge with Dirichlet boundary conditions, we can insert two tachyon vertices. The amplitudes in this case are given by (see Fig.3)

$$I_2^{(1)}(k_1, k_2; t) = {}_{NN}^{D} \langle B^o | q^{L_0^{NN} - \frac{1}{24}} | B^o; k_1, k_2 \rangle_{NN}^N$$

$$= 2^{\frac{\widetilde{12}}{2}} e^{-i(k_1 + k_2)x} \left(\frac{\eta(t)}{\eta(2t)} \right)^{\frac{1}{2}} \left(\frac{\eta(2t)^2}{\eta(t)} \right)^{\frac{\widetilde{1}^2 + \widetilde{2}^2}{2}} \left(\frac{\eta(4t)^2 \eta(t)}{\eta(2t)^3} \right)^{\widetilde{12}}, \tag{5·11}$$

$$I_2^{(2)}(k_1; k_2; t) = {}_{DN}^{N} \langle B^o; k_2 | q^{L_0^{ND} + \frac{1}{48}} | B^o; k_1 \rangle_{ND}^N$$

$$= e^{-i(k_1 + k_2)x} \left(\frac{\eta(t)}{\eta(t/2)} \right)^{\frac{1}{2}} \left(\frac{\eta(t/2)^2}{\eta(t)} \right)^{\frac{\widetilde{1}^2 + \widetilde{2}^2}{2}} \left(\frac{\eta(t/4)^2 \eta(t)}{\eta(t/2)^3} \right)^{\widetilde{12}}. \tag{5·12}$$

These are related by the modular transformation

$$I_2^{(1)}\left(k_1, k_2; \frac{1}{t}\right) = 2^{\frac{1}{4}-\frac{\widetilde{1}^2+\widetilde{2}^2}{2}} t^{\frac{1}{4}(\widetilde{1}^2+\widetilde{2}^2)} I_2^{(2)}(k_1; k_2; t), \qquad (5\cdot13)$$

which is graphically depicted in Fig.4 (b). We can extract the weight of the renormalized vertex from the term $t^{\frac{1}{4}(\widetilde{1}^2+\widetilde{2}^2)}$. The two-tachyon amplitudes (5·13) possess the exact modular property up to the extra factor $2^{\frac{1}{4}-\frac{\widetilde{1}^2+\widetilde{2}^2}{2}}$, but this extra factor can be absorbed in the redefinition of the boundary state. The weight of the renormalized vertices is then identified with $\frac{1}{4}(\widetilde{1}^2 + \widetilde{2}^2)$. In this case, the total intrinsic weight vanishes, which is clear from the assignment of the boundary conditions.

One tachyon insertion

In the case that two adjacent edges have Neumann boundary conditions and the other two edges have Dirichlet boundary conditions, we can insert only one tachyon vertex (see Fig.3):

$$I_1(k; t) = {}^D_{DN}\langle B^o|q^{L_0^{ND}+\frac{1}{48}}|B^o; k\rangle^N_{ND}$$
$$= e^{-ikx}\left(\frac{\eta(2t)\eta(t/2)}{\eta(t)^2}\right)^{\frac{1}{2}}\left(\frac{\eta(t)^5}{\eta(2t)^2\eta(t/2)^2}\right)^{\frac{\widetilde{k}^2}{2}}. \qquad (5\cdot14)$$

Its modular property is

$$I_1\left(k; \frac{1}{t}\right) = t^{\frac{\widetilde{k}^2}{4}} I_1(k; t), \qquad (5\cdot15)$$

which is graphically depicted in Fig.4 (c). This reproduces the weight of the renormalized vertex $\frac{\widetilde{k}^2}{4}$. The intrinsic weight vanishes again in this case, due to the assignment of boundary conditions.

§6.   Conclusion

In this paper, we introduced the boundary state in the open string channel for a free boson and a fermionic ghost. Their inner product gives a string amplitude on a rectangle. We carefully studied the CFT near the corner carefully and elucidated certain nontrivial features, such as the correction of the weight of primary fields.

There are many important issues which we did not address in this paper. One of the most important problems is to generalize our treatment to other CFT, for example, the minimal model,[5] the orbifold,[9] the Wess-Zumino model,[10] and of course superstrings.[1,2] OBS for the Majorana fermion is somehow nontrivial, because the naive analog of the fermionic ghost, $e^{\frac{\pm i}{2}\sum_{r>0}(\psi_{-r})^2}|0\rangle$, is meaningless. In order to resolve this problem, we have to be careful in treating the singularity at the corner. The behavior of fermion fields must be considered in order to determine how two D-branes can intersect.

Another important problem is to determine the proper normalization of the open boundary state. For the boundary states of a closed string, it is fixed by the modular property (Cardy condition)[18] and can be interpreted as the boundary entropy[19] in

statistical mechanics or the tension of the D-brane in string theory.[11] This is closely related to the generalization to generic CFT and is a very important problem in the study of string dynamics.

We are also interested in the classical field configuration near the D-brane. For a closed string, it is known[3] that classical supergravity solutions near the D-brane can be constructed from the massless part of the boundary state. It may be thought that, just as in the closed string case, we can reproduce the soliton profile for source D-branes dissolved in higher-dimensional D-branes by extracting the massless part in the OBS. We note that an analysis similar in spirit to that described here is carried out in Refs. 20) and 21) for D3-D(-1) systems, although the idea of OBS is not introduced there. The authors of these works computed a disk amplitude that is equivalent to $\langle P|q^{L_0}|B^o\rangle$ in our language, where $\langle P|$ is a massless state of open strings on D3-branes and $|B^o\rangle$ is the OBS for D(-1)-branes. They showed that this amplitude actually reproduces the instanton profile on D3-branes. If we can translate their computation into OBS language, it would support the conclusion that OBS can be interpreted as describing a soliton configuration in gauge theory. This would provide further confirmation of the relevance of OBS.

We finally mention that OBS appear in the context of string field theory[12] (see also Refs. 22) and 13)) and are used in defining the modular dual description of Witten's string field theory. They define the on-shell external state in such a formulation and directly define the D-brane as a solution to string field theory. Determining the role played by the boundary state as a solution to the second quantized theory continues to be a challenging problem.

References

1) C. G. Callan, C. Lovelace, C. R. Nappi and S. A. Yost, Nucl. Phys. B **288** (1987) 525 ; Nucl. Phys. B **293** (1987) 83 ; Nucl. Phys. B **308** (1988) 221.
2) J. Polchinski and Y. Cai, Nucl. Phys. B **296** (1988) 91.
3) P. Di Vecchia and A. Liccardo, NATO Adv. Study Inst. Ser. C. Math. Phys. Sci. **556** (2000) 1, [arXiv:hep-th/9912161].
4) P. Di Vecchia and A. Liccardo, [arXiv:hep-th/9912275].
5) R. E. Behrend, P. A. Pearce, V. B. Petkova and J. B. Zuber, Nucl. Phys. B **570** (2000) 525 [Nucl. Phys. B **579** (2000) 707] [arXiv:hep-th/9908036].
6) J. Fuchs and C. Schweigert, Nucl. Phys. B **558** (1999) 419 [arXiv:hep-th/9902132]; Nucl. Phys. B **568** (2000) 543 [arXiv:hep-th/9908025].
7) J. Frohlich, O. Grandjean, A. Recknagel and V. Schomerus, Nucl. Phys. B **583**, 381 (2000) [arXiv:hep-th/9912079].
8) M. R. Gaberdiel, Class. Quant. Grav. **17** (2000) 3483 [arXiv:hep-th/0005029].
9) M. Billo, B. Craps and F. Roose, JHEP **0101** (2001) 038 [arXiv:hep-th/0011060].
10) V. Schomerus, Class. Quant. Grav. **19** (2002) 5781 [arXiv:hep-th/0209241].
11) J. Polchinski, Phys. Rev. Lett. **75** (1995) 4724 [arXiv:hep-th/9510017].

12) H. Isono and Y. Matsuo, [arXiv:hep-th/0511203].

13) A. Ilderton and P. Mansfield, Phys. Lett. B **607** (2005) 294, [arXiv:hep-th/0410267]; JHEP **0510** (2005) 016, [arXiv:hep-th/0411166].

14) M. Cvetic and I. Papadimitriou, Phys. Rev. D **68** (2003) 046001 [Erratum-ibid. D **70** (2004) 029903] [arXiv:hep-th/0303083].

15) S. A. Abel and A. W. Owen, Nucl. Phys. B **663**, (2003) 197 [arXiv:hep-th/0303124]; Nucl. Phys. B **682**, (2004) 183 [arXiv:hep-th/0310257].

16) D. J. Gross and A. Jevicki, Nucl. Phys. B **283** (1987) 1 ;   Nucl. Phys. B **287** (1987) 225.

17) O. Alvarez, Nucl. Phys. B **216** (1983) 125;
A. M. Polyakov, Phys. Lett. B **103** (1981) 207; Phys. Lett. B **103** (1981) 211.

18) J. L. Cardy, Nucl. Phys. B **324** (1989) 581.

19) I. Affleck and A. W. W. Ludwig, Phys. Rev. Lett. **67** (1991) 161.

20) M. Billo, M. Frau, F. Fucito, A. Lerda, A. Liccardo and I. Pesando, JHEP **0302** (2003) 045, [arXiv:hep-th/0211250].

21) M. Frau and A. Lerda, Fortsch.Phys. **52** (2004) 606, [arXiv:hep-th/0401062].

22) D. Gaiotto, L. Rastelli, A. Sen and B. Zwiebach, JHEP **0204** (2002) 060, [arXiv:hep-th/0202151].